Adaptive Rate Control in High-Speed Networks: Performance Issues *

Mohamed Abdelaziz†[†] Ioannis Stavrakakis ‡

†Core Switching Division
Lucent Technologies
1 Robbins Rd.,
Westford, MA 01886
Email: mza1@lucent.com

‡Department of Informatics and Telecommunications
University of Athens
Panepistimiopolis, Ilisia, 157-84
Athens, Greece
Email: istavrak@di.uoa.gr

Abstract

It is well established that increased network transmission speed reduces the effectiveness of feedback-based adaptive rate control mechanisms, due to the increased bandwidth propagation delay product. In this environment, differences in the propagation delays associated with the controlled sources become larger when measured in slots (transmission time of information unit), potentially inducing substantially diversified performance metrics. One of the objectives in this work is to quantify the potential unfairness as well as the reduced effectiveness of this rate control scheme in the presence of non-zero propagation delays. As the network speed increases, it is also expected that traffic sources will seem to be slower due to the relative increase of the information generation time and/or the decrease of the portion of the bandwidth required by a specific source. The other objective in this work is to investigate and quantify the expected increased effectiveness of this rate control scheme in the presence of non-zero propagation delays as the traffic sources become slower. The studies are carried out by formulating queuing models and evaluating the per-session cell loss probabilities and they are supported by numerical results.

*Research supported in part by the Advanced Research Project Agency under Grant F49620-93-1-0564 monitored by the Air Force Office of Scientific Research (AFOSR).

[†]Dr. Abdelaziz's work was done while he was at the University of Vermont

1 Introduction

Traditionally, packet-switched data networks have provided a best-effort type of service without guaranteeing the provided Quality of Service (QoS). Bandwidth is shared by the different traffic sources in the network in a dynamic manner and no explicit limits are imposed on the amounts of the traffic entering the network. In contrast, circuit-switched public telecommunication networks have employed fixed peak bandwidth allocation techniques, enabling the provisioning of QoS guarantees by limiting the input traffic at the connection set-up phase. While traffic management schemes used in packet switching networks provide the potential for efficient network utilization and those used in circuit-switched networks provide QoS guarantees, neither can cope alone with the requirement of guaranteeing the provided QoS while attaining efficient utilization of resources in ATM networks.

Unlike circuit-switched telecommunication networks and packet-switched data networks where a certain type of service is primarily supported, B-ISDN ATM networks are expected to support a multitude of services with diverse characteristics and quality of service requirements. In order to guarantee the QoS of the supported applications, a preventive traffic management approach has been primarily considered [1]. During the call set-up phase the associated traffic source provides a set of traffic descriptors and QoS requirements. The call is admitted if — based on the provided information and the current network conditions — it is determined that the QoS of this call as well as that of existing ones can be delivered. In addition, traffic shaping schemes are employed to smooth the traffic and allow its representation in terms of properly identified traffic descriptors; traffic policers enforce the compliance of the traffic delivered to the network to the adopted traffic descriptors. This (preventive) traffic management approach provides QoS guarantees to individual calls by properly shaping the call's traffic and limiting the number of calls that can be supported at any given time. Such an approach is necessary to guarantee the QoS requirements of voice and video services which require very low cell loss probabilities and stringent bounds on cell delays and cell delay variation.

In order to accommodate the delay tolerant applications whose traffic may not be possible to specify at call set-up — for instance, ABR (Available Bit Rate) and UBR (Unspecified Bit Rate) applications [2], [3] — adaptive feedback-based rate control schemes have been proposed. Through dynamic sharing of the available [1] network capacity, increased network utilization may

[1]The available network capacity may be defined at any of 3 levels determined by the time-scale involved: on a semi permanent basis determined by the network management, on a call level basis or instantaneously [4]. Examples of semi-permanent allocations may include dedicated virtual paths that are changed over the time-scale of days/months. On

be achieved.

Adaptive, feedback-based mechanisms were first introduced to dynamically control the user's traffic (sending windows at the transport layer level) in classical packet switched networks [5]. Examples include the DECBit rate adjustment scheme [6] and the slow start enhancement to the TCP/IP [7]. Similar concepts have been proposed ([8], [9], [10], [11], [12]) to directly control the rate of traffic sources where rates are either determined explicitly by some network controllers [11] or are incremented and decremented in an adaptive fashion based on some fed-back network information [13], [14], [15]. Applications of such adaptive schemes for the control of voice/video coders can be found in [16] and [17].

Due to the large bandwidth propagation delay product characterizing high-speed networks (such as ATM), network feedback information may be outdated by the time it reaches a source. Thus, it is necessary to evaluate the performance of such adaptive control schemes in high-speed networking environments. Since the Quality of Service (QoS) of many applications is often expressed in terms of very low loss probabilities, a performance evaluation approach based on the prevalent standard simulation techniques is becoming less formidable. For this reason, studies based on analytically tractable techniques are becoming of great importance. Several studies have shown that adaptive rate control schemes are adversely affected by the presence of propagation delays between the controlled sources and the control nodes [18] and several authors have limited the applicability of such schemes to the realm of local area networks [19], [20] where propagation delays are no longer than several tens of the service time.

Unlike in open-loop schemes where no competition for network bandwidth takes place once a call is set-up, an important characteristic of adaptive rate control schemes is that existing connections compete, at the cell level, for the available bandwidth. This competition may result in unfair allocation of the resources and some mechanisms may be necessary to establish fairness. Fairness is defined in this work in the sense that equal performance measures are delivered to the different connections within the same class. The issue of fair allocation of resources under adaptive rate control schemes is considered in [21] in the presence of negligible propagation delays and in [22] where all controlled sources have the same propagation delays. In ATM networking environments where geographically dispersed areas are spanned by the supported services, it is not uncommon that sources located at significantly different physical distances

the call level, the available bandwidth for the ABR service fluctuates as guaranteed QoS calls (e.g. video and voice) are established and released. Finally, capacity may become available to ABR applications due to instantaneous fluctuations of the traffic during the lifetime of a guaranteed QoS call.

share the same network access node. Since the effectiveness of adaptive rate control schemes is known to be affected by the propagation delays, it is expected that some unfairness may arise in this environment. In order to quantify the resulting unfairness, it is necessary to be able to isolate the performance of individual sessions subject to adaptive rate control. Due to the associated analytical difficulty, most previous analytical studies for adaptive rate control schemes have focused on aggregate performance measures.

In addition to the large bandwidth propagation delay products characterizing high-speed networks, an often overlooked — by earlier discrete-time studies such as [20], [14] — characteristic is the potentially large disparity between the relative speeds of a network link and an input source. This disparity or speed-up factor represents the time *in slots* required for a source to generate enough bits to form one cell [2] and is referred to as the source time constant [23]. Notice that both the bandwidth propagation delay product and the time between consecutive cell transmissions from the same source increases as the network link speed increases. And while the former indicates the existence of larger traffic volume in the pipe (in transit), the latter indicates the existence of a lower traffic volume in the pipe coming from the same source. While both these factors clearly influence the performance of an adaptive rate control scheme, only the first has been considered in most previous studies.

In section 2, the impact of an increased source time constant on the effectiveness of the adaptive feedback-based rate control under non-zero propagation delays is investigated. Unlike previous considerations, the time-constant of the sources is assumed to be greater than one (network slot). As a result, cells can not be generated over consecutive time-slots whose distance is less than the sources time-constant. The considered queuing model also allows for the performance evaluation of adaptively controlled connections with significantly different propagation delays and can be viewed as a generalization of those considered in [20],[24] and can reduce to any of those models by proper parameter setting. This model may be adopted to model a switching node of a high speed network receiving traffic from lower speed networks or from sources with slow cell generating mechanisms compared to the network time constant (slot). As established in section 2, the greatest reduction in the effectiveness of the adaptive rate control, due to non-zero propagation delays, will be experienced by sources with the smallest time constant (one slot). For this reason — as well as because of sources with time constant one has been considered in almost the entire past work — the study in section 3 is carried out for sources with time

[2] Similarly, a time constant can be defined as the minimum spacing among consecutive blocks of consecutive cells generated by a source which is required to receive (generate) an entire packet before cells are created.

constant one. The magnitude of the impact of the diversified non-zero propagation delays is expected to be reduced in the presence of the slower sources. Finally, some concluding remarks are presented in section 4.

2 Adaptive Rate Control for Slow Sources

The model considered in this work is shown in Fig. 1 where a number of sources share a common network access node. The access node is modeled by a finite buffer receiving deterministic service. Sources are assumed to be located at the same physical distance from the network access node and, thus, have the same propagation delays.

Under an adaptive rate control mechanism, a traffic descriptor to be modulated is identified (for instance, the arrival rate) and sources adjust its value dynamically, based on either explicit or implicit information about the state of the network. The network state is determined in terms of some pre-identified state descriptor such as the node load or buffer occupancy. By comparing the state descriptor to a threshold value, the network state is determined to be in either an underload or an overload state.

The network state is reviewed periodically over intervals of length T_u, referred to as update intervals. At the end of each update interval, the network state is communicated to the traffic sources. Either the same or different update intervals may be used to update the sources sharing the network node. Individual sources receive the network state information after a time interval equal to their respective propagation delays and respond by modulating the pre-identified traffic descriptor. The modulated traffic is received at the network node a round-trip propagation delay time after the network state information is sent. The tradeoffs involved in the choice of the length

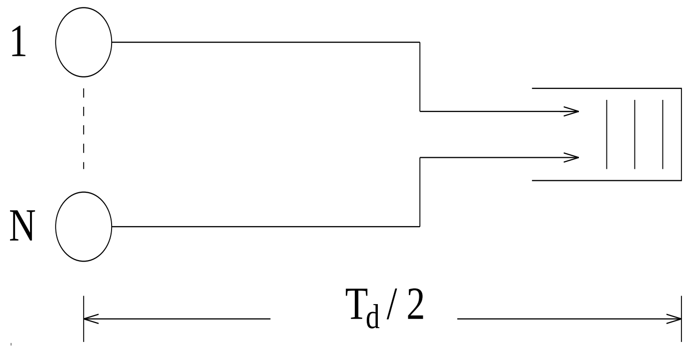

Figure 1: Queuing model for the study of the impact of the source time constant on the effectiveness of the adaptive rate control.

of the update interval can be found in [4]; the impact of the selected update interval on the performance of the individually controlled connections will be considered in section 3. In this section, all sources are assumed to be updated according to the same update interval which is equal to the round trip propagation delay ($T_u = T_d$).

In this work, sources modulate their (instantaneous) transmission rates based on the state of the network buffer. A two-level (Binary) adaptation scheme is considered, where sources switch to a high arrival rate (λ_1) if the network is underloaded and switch to a low arrival rate (λ_0) if the network is overloaded. Notice that an additive increase multiplicative decrease rate control system may not be exactly implementable by most switching architectures due to the floating points multiplications required in decreasing the rates of individual virtual circuits and the inherent associated scheduling difficulties. A typical implementation may use built-in tables of possible arrival rates corresponding to an M-level adaptive rate scheme. The two level scheme ($M = 2$) presented in this paper is chosen for tractability, and to help gain insight into the associated design and performance issues. The precise description of the arrival process considered in this section is presented in the following subsection.

2.1 The Arrival Process

Arrivals from the l^{th} controlled source can be represented by a two state process $\{r^l\}, r^l \in \{0, 1\}$ and is specified by the set of parameters $\{T_c^l, f_i^l(k) : 0 \leq i \leq 1\}$. T_c^l is an integer constant which represents the minimum time between consecutive arrivals (potential arrival instants) from the l^{th} source and will be referred to as the time constant of the l^{th} source; $f_i^l(k)$ denotes the probability mass function (PMF) for the number of cells generated at potential arrival instants (boundaries separated by the time constant) when the arrival process of the l^{th} source is in state $i, i \in \{0, 1\}$. State transitions for the arrival process are governed by the two-level adaptive rate control mechanism — as determined by the state of the network-state descriptor fed back to the individual sources — and occur at time instants coinciding with the boundaries of the update intervals.

Note that by appropriately choosing T_c, the considered source model is capable of modeling the cell arrival dynamics at different time scales. For instance, setting $T_c = 1$ leads to the regular arrival processes considered in [20]. Also, setting $f_0^l(k) = f_1^l(k)$ leads to the non-deterministic periodic arrival process considered in [24].

In addition to the above parameters, let c^l, $1 \leq c^l \leq T_c$, denote the time instant at which the l^{th} source is activated. c^l represents the phase difference between the different arrival processes and will be referred to as the initialization time of the l^{th} source. N such source with the same time constant T_c are said to be fully synchronized if $c^1 = \cdot\cdot = c^N$.

The aggregate arrival process from N synchronized sources with time constants $T_c^j = k_j \min\{T_c^j\}$, $0 \leq j \leq N$ can be completely described by the parameters $\{T_c, F_i(.) : 0 \leq i \leq 1\}$ where $T_c = \mathrm{LCM}\{T_c^j\}$ (the Least Common Multiple) and $F_i(.)$ is the N-fold convolution of the individual PMFs $f_i(.)$. N_i and λ_i will be used to denote the maximum number of cell arrivals per slot and the average arrival rate from state i of the aggregate arrival process, respectively.

2.2 Queuing Analysis

In this subsection, the queuing analysis is carried out in discrete-time. Time is slotted and a slot duration is equal to the transmission time of one cell. Although the provided analysis can be used to study sources with different time constants, all N sources considered will be assumed to have the same time constant T_c and the same propagation delay T_d in order to facilitate the presentation and the discussion of the numerical results. The round-trip propagation delay T_d is assumed to be an integer multiple of the time-constant T_c, that is, $T_d = M \times T_c$, $M \in Z^+$, where Z^+ is the set of positive integers. Similar analysis can be adopted for the case $T_c = M \times T_d$, $M \in Z^+$.

Time is divided into frames of length T_d slots; each frame is divided into M subframes, each of length T_c slots. Cell arrivals from the controlled sources arrive at a finite size network buffer of capacity Q and are served according to the FIFO service policy. Arrivals from individual sources occur at subframe boundaries and are assumed to follow a Bernoulli PMF with rate α_1 when in state 1 and rate α_0 when in state 0. Therefore, the aggregate arrival process at subframe boundaries is Binomial with parameters N, α_1 (N, α_0) when in state 1 (0). The aggregate arrival rate from state 1 (0) is $\lambda_1 = \frac{N\alpha_1}{T_c}$ $(\lambda_0 = \frac{N\alpha_0}{T_c})$.

Let $\{q_k\}_{k\geq 0}$ be the buffer occupancy process embedded at subframe boundaries with state space $S^Q = \{0, 1, \cdots, Q\}$. Let q_{th} be the buffer threshold value indicating the network state as overloaded $(q \geq q_{th})$ or underloaded $(q < q_{th})$. Let $\{r_k\}_{k\geq 0}$ be the arrival process embedded at the subframe boundaries with state space $S = \{0, 1\}$. Note that since the duration of the frame is equal to the duration of the update interval (T_d slots), state transitions of the process $\{r_k\}_{k\geq 0}$ occur only at *frame* boundaries. Due to the propagation delay, the state of process $\{r_k\}_{k\geq 0}$ at the beginning of frame k is determined by the state of the buffer process at the beginning of frame $k-1$. Thus, the arrival process evolves as follows:

$$r_{k+1} = \begin{cases} 1 & \text{if} \quad q_k < q_{th} \\ 0 & \text{if} \quad q_k \geq q_{th} \end{cases}$$

The system state can be defined at frame boundaries in terms of the quantities (r_k, q_k). Given that $r_k = i$ at the beginning of frame k, the finite queue will evolve over frame k under the i.i.d. batch arrival process with PMF $F_i(\cdot)$. It is easy to establish that the stochastic process $\{r_k, q_k\}_{k\geq 0}$, embedded at frame boundaries, is a finite state Markov chain with state space $S_p = \{(r_1, q_1) : 0 \leq r_1 \leq 1, 0 \leq q_1 \leq Q\}$

The probability that the Markov chain moves from state (r_1, q_1) at the beginning of the k^{th} frame to state (r_2, q_2) at the beginning of the $(k+1)^{st}$ frame will be denoted by $p(r_1, q_1, r_2, q_2)$ and can be evaluated recursively as follows:

$$p(r_1, q_1, r_2, q_2) = \begin{cases} 0 & \text{if } (q_1 < q_{th}), (r_2 = 0) \\ 0 & \text{if } (q_1 \geq q_{th}), (r_2 = 1) \\ p_{r_1}^M(q_1, q_2) & \text{otherwise} \end{cases} \tag{1}$$

where $p_{r_1}^M(q_1, q_2)$ denotes the probability that the process $\{q_k\}_{k\geq 0}$ moves from state q_1 to state q_2 in M subframes under the assumption that process $\{r_k\}_{k\geq 0}$ remains unchanged over this transition. The i.i.d. arrivals — occurring at the subframe boundaries — will be determined by the PMF $F_{r_1}(\cdot)$. $p_{r_1}^M(q_1, q_2)$, $0 \leq q_1, q_2 \leq Q$ — called the M-subframe-step transition probability under state r_1 — are easily calculated in terms of the 1-subframe-step transition probabilities $p_{r_1}^1(q_1, q_2)$, $0 \leq q_1, q_2 \leq Q$ which are derived as follows. Consider the following definitions:

$\tilde{p}_{r_1}^1(q_1, l)$: denotes the probability that the buffer occupancy process moves from state q_1 to state l over the first slot of a subframe under state r_1, $r_1 \in \{0, 1\}$, $0 \leq q_1, l \leq Q$.

$\tilde{p}^2(l, q_2)$: denotes the probability that the buffer occupancy process moves from state l at the end of the first slot of the current subframe to state q_2 at the end of the current subframe ($0 \leq l, q_2 \leq Q$). Notice that no arrivals can occur during this transition due to the source time constant and that the buffer occupancy can only decrease.

Then the 1-subframe-step transition probabilities $p_{r_1}^1(q_1, q_2)$, $0 \leq q_1, q_2 \leq Q$, are given by:

$$p_{r_1}^1(q_1, q_2) = \sum_{l=0}^{Q} \tilde{p}_{r_1}^1(q_1, l)\tilde{p}^2(l, q_2)$$

where $\tilde{p}^2(l, q_2)$, $0 \le l, q_2 \le Q$, are given by:

$$\tilde{p}^2(l, q_2) = \begin{cases} 0 & \text{if} \quad q_2 \ge 1, (l - q_2 \ne T_c - 1) \\ 1 & \text{if} \quad q_2 \ge 1, (l - q_2 = T_c - 1) \\ 1 & \text{if} \quad q_2 = 0, (l \le T_c - 1) \end{cases}$$

and $\tilde{p}^1_{r_1}(q_1, l)$, $r_1 \in \{0, 1\}$, $0 \le q_1, l \le Q$, are given by:

$$\tilde{p}^1_{r_1}(q_1, l) = F_{r_1}(l - q_1 + 1) + F_{r_1}(0) \cdot \mathbf{1}_{\{q_1 + l = 0\}}, \; 0 \le q_1 \le Q, \; \max(0, q_1 - 1) \le l \le Q - 1$$

$$\tilde{p}^1_{r_1}(q_1, Q) = \sum_{l = Q - q_1 + 1}^{N_{r_1}} F_{r_1}(l)$$

where $\mathbf{1}_{\{q_1 + l = 0\}}$ is an indicator function that takes the value 1 if $q_1 + l = 0$ and takes the value 0 otherwise, and N_{r_1} denotes the maximum number of arrivals, as determined by the state of the aggregate cell arrival process, r_1.

The stationary probabilities of the Markov Chain $\{r_k, q_k\}$ ($\pi(r_1, q_1)$, $r_1 \in \{0, 1\}, 0 \le q_1 \le Q$) can be easily computed by solving the system of linear equations $\{P\Pi = \Pi, \; \Pi e' = 1\}$, where P is the transition probability matrix with elements given by (1), Π is the stationary probability vector and e is the unity vector.

It should be noted that since the Markov chain $\{r_k, q_k\}$ is embedded at the frame boundaries, the complexity in computing its stationary probabilities by solving the system of equations $\{P\Pi = \Pi, \; \Pi e' = 1\}$ is independent of T_d. As a consequence, systems with relatively large propagation delays may be considered without significant numerical complexity. A large value of T_d, however, may indirectly impact on the numerical complexity through the number of subframes M, but the potential complexity in calculating the $M - step$ transition probabilities is not the limiting factor of the presented numerical approach.

2.3 Cell Loss Probability

In this subsection, the cell loss probability of an arbitrary arriving cell is derived. In the following, let r_1 be the state of the arrival process at the beginning of the current frame. Let q_1 be the buffer state at the beginning of the k^{th} subframe in the current frame. Let $w_f(r_1, i, k), 1 \le k \le M$ be a random variable describing the number of cells lost over the period starting from the beginning of the k^{th} subframe till the end of the current frame (over a period of $M - k$ subframes). Clearly, $w_f(r_1, q_1, 1)$ describes the number of losses over a period of a frame.

It can be easily shown that the loss probability (L) can be derived in terms of the expected value of $w_f(.,.,1)$, $\overline{w_f}(.,.,1)$, as follows:

$$L = \frac{\sum_{(r_1,q_1)\in S_p} \pi(r_1,q_1)\overline{w_f}(r_1,q_1,1)}{\sum_{(r_1,q_1)\in S_p} \pi(r_1,q_1)\lambda_{r_1} T_d}$$

The random variables $w_f(r_1,q_1,k)$, $1 \leq k \leq M$, $(r_1,q_1) \in S_p$ and their expected values can be derived recursively by noting that the number of cells lost starting from the k^{th} subframe in the current frame till the end of the frame is equal to the number of cells lost over the k^{th} subframe plus the number of cells lost from the beginning of the $(k+1)^{st}$ subframe till the end of the frame. Let $w_s(r_1,q_2)$ be a random variable describing the number of cells lost during the k^{th} subframe at the beginning of which the buffer occupancy is q_2, $(r_1,q_2) \in S_p$. Then:

For $q_1, q_2 \in \{0,\cdots,Q\}, r_1 \in \{0,1\}$, $1 \leq k \leq M-1$:

$$w_f(r_1,q_1,k) = w_s(r_1,q_1) + w_f(r_1,q_2,k+1) \quad \text{with probability} \quad p^1_{r_1}(q_1,q_2),$$

and

$$w_f(r_1,q_1,M) = w_s(r_1,q_1).$$

The probabilities $p^1_{r_1}(q_1,q_2)$ were computed in section 2.2. The random variables $w_s(.,.,.)$ needed for the computation of $w_f(.,.,.)$ can be evaluated as follows. Let a_1 denote a random variable describing the number of arrivals over the first slot of the subframe.

For $r_1 \in \{0,1\}, q_1 \in \{0,\cdots,Q\}$,:

$$w_s(r_1,q_1) = \begin{cases} (l-Q+q_1-1) & \text{if } a_1 = l, (Q-q_1+1) \leq l \leq N_{r_1} \\ 0 & \text{otherwise} \end{cases}$$

By considering the expectation of the above equations, the following are obtained:

$$\overline{w}_s(r_1,q_1) = \sum_{l=Q-i+1}^{N_{r_1}} (l-Q+q_1-1).F_{r_1}(l)$$

For $q_1, \in \{0,\cdots,Q\}, r_1 \in \{0,1\}$, $1 \leq k \leq M-1$:

$$\overline{w}_f(r_1,q_1,k) = \overline{w}_s(r_1,q_1) + \sum_{q_2} p^1_{r_1}(q_1,q_2)\overline{w}_f(r_1,q_2,k+1) \tag{2}$$

and

$$\overline{w}_f(r_1,q_1,M) = \overline{w}_s(r_1,q_1) \tag{3}$$

By computing $\overline{w}_f(r_1,q_1,M)$, from (3), and back substituting in (2), $\overline{w}(r_1,q_1,1)$ can be obtained.

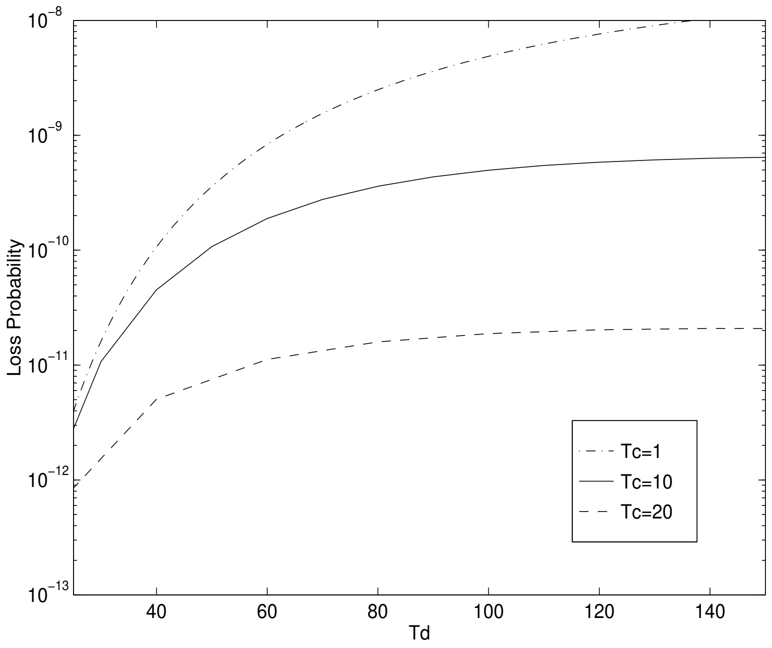

Figure 2: Loss Probability versus the propagation delay for various source time constants

2.4 Numerical Results and Discussion

The numerical results presented in this section are derived assuming 2-state Markov modulated Binomial arrivals at subframe boundaries with parameters $(N, \lambda_0/N)$ under state 0 and $(N, \lambda_1/N)$ under state 1.

The induced cell loss probability as a function of the round-trip propagation delay T_d for various values of the common source time constant T_c are shown in Fig. 2. The results have been obtained for $\lambda_1 = 0.9$, $\lambda_0 = 0$, $Q = 70$, $q_{th} = 40$ and $N = 40$. As expected (and established in past research), the effectiveness of the adaptive feedback-based rate control decreases as T_d increases, as indicated by an increased value of the induced cell loss probability. The results also indicate that for a fixed value of T_d, the effectiveness of this control scheme increases as the source time constant increases. This implies that the performance of an adaptive feedback-based rate control scheme may be substantially underestimated if the time constant of the arrival process is assumed to be one ($T_c = 1$). Considering a different point of view, assuming $T_c = 1$ for slow sources may limit the range of applicability of this rate control scheme. For instance, this rate control policy can guarantee a cell loss probability of 10^{-9} only if $T_d \leq 60$ if $T_c = 1$, while the same policy will still provide the same cell loss probability guarantee for much higher values of T_d ($T_d \geq 150$) for $T_c = 10$. This range is further extended for lower values of T_c.

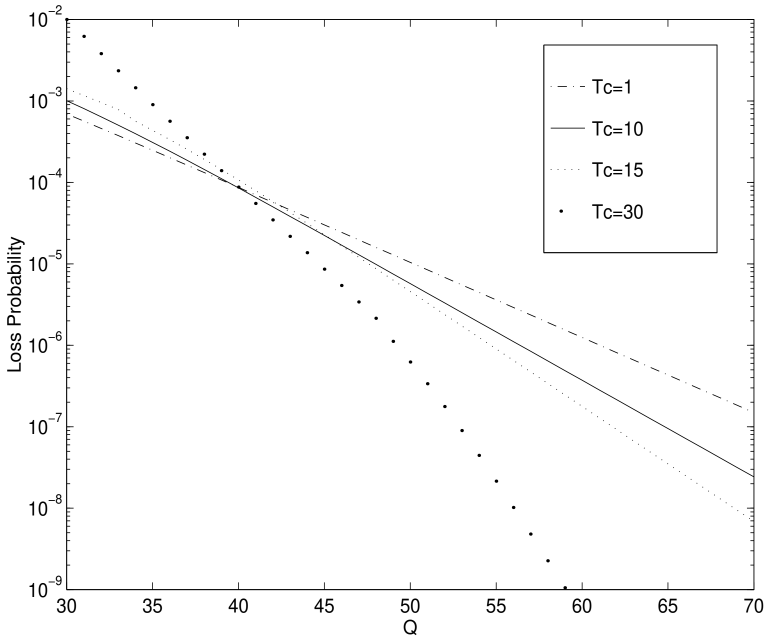

Figure 3: Loss probability versus buffer capacity for various source time constants

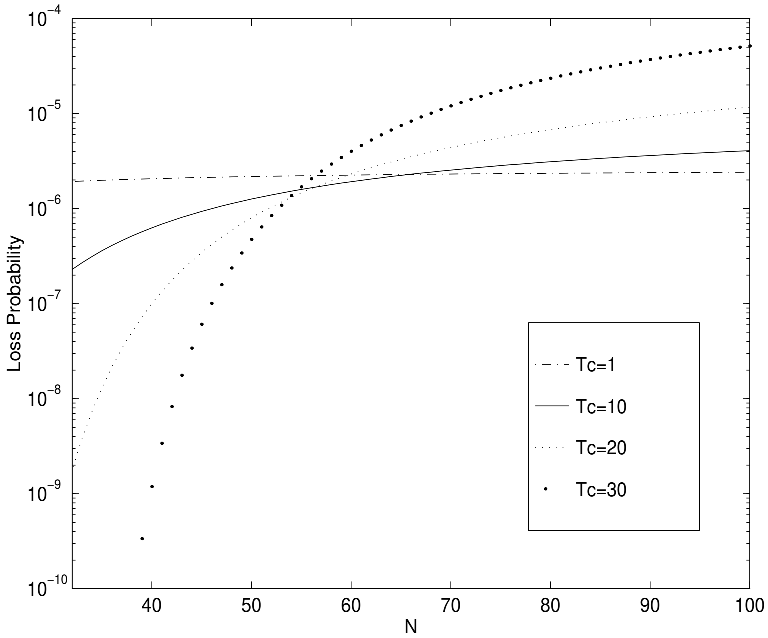

Figure 4: Loss probability versus the number of controlled sources for various source time constants

This behavior can be explained by noticing that there are two primary sources for cell loss in the considered model: the first is the traffic in transition (in the feedback loop/pipe) that may overflow the buffer after the queue threshold is exceeded while sources switch to the lower arrival rate. The second is the arrival of batches of cells separated by the time constant of the arrival process. One, or the other, of the cell loss components induced by the above two sources may dominate depending on the time constant of the arrival process and the available buffer size. A slow process (larger T_c) having the same arrival rate as that of a faster process (shorter T_c) submits larger batches separated by its "larger" time constant. Consequently, if the available buffer size is not large enough to accommodate the larger batches, the losses induced due to the batch arrivals from the slower process will be more significant than that induced by a process having smaller batches. For larger buffer sizes however, the batch loss component is absorbed by the available buffer sizes and the cell losses are primarily due to the traffic in the pipe. This traffic is less from a slower process and therefore the lower losses and the observed improved effectiveness of the adaptive rate control.

The impact of the buffer capacity Q and the source time constant T_c on the induced cell loss probability is shown in Fig. 3 for a fixed value of $T_d = 30$; the other parameters were set to $\lambda_1 = 0.94$, $\lambda_0 = 0.9$, $q_{th} = 20$ and $N = 40$. Notice that for $T_c > 1$, the effectiveness of the adaptive rate control scheme can either increase or decrease compared to that for $T_c = 1$. When the buffer capacity is less than N (approximately) the effectiveness of the adaptive rate control scheme decreases as the source time constant increases. The opposite behavior is observed for buffer capacity values exceeding (approximately) N. In view of the fact that the number of sources coincides with the maximum value of the cell batch size, it may be concluded that as long as sufficient buffer space is available to absorb a single batch (called *batch-absorption buffer capacity value*), the effectiveness of the adaptive rate control will increase as the source time constant increases. Considering a different point of view, a fixed increase in the buffer capacity (for a fixed value of T_d and buffer capacities exceeding the batch-absorption value) will result in much larger improvement of the effectiveness of the adaptive rate control scheme for slower sources.

The impact of the number of controlled sources N and the source time constant T_c on the induced cell loss probability is shown in Fig. 4, for $T_d = 30$. The other parameters were set to $Q = 50$, $\lambda_1 = 0.94$, $\lambda_0 = 0.9$, $q_{th} = 30$. The same conclusions can be drawn here as from Fig. 3. When N is (approximately) less than Q, the effectiveness of the adaptive rate control scheme increases as the source time constant increases . The effectiveness decreases when N

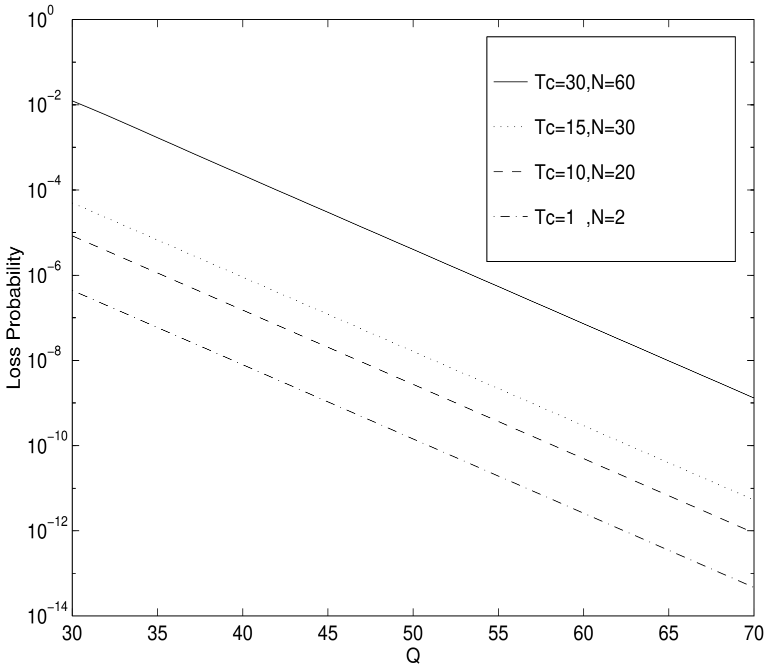

Figure 5: Impact of Source Synchronization

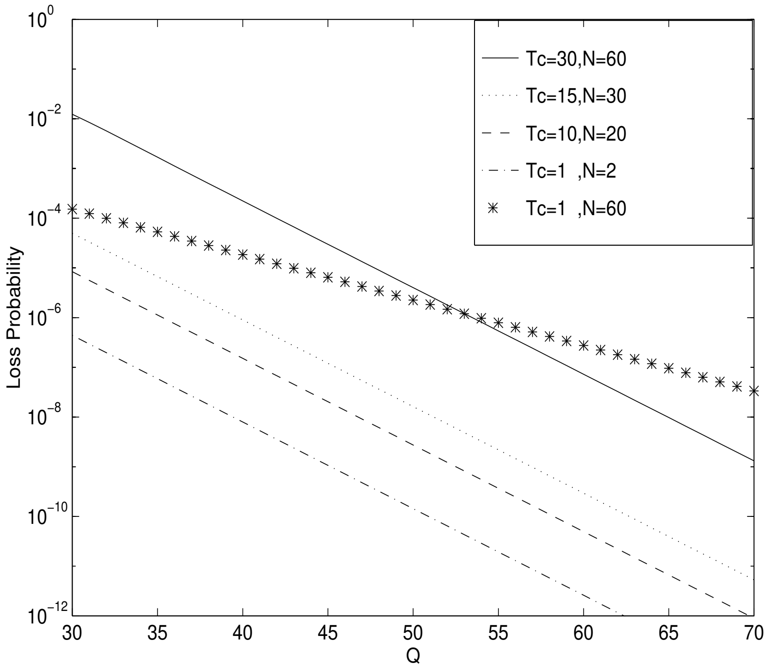

Figure 6: Impact of Source Synchronization

(approximately) exceeds Q. One significant conclusion from these results is that for a fixed cell loss probability and (sufficiently large) fixed buffer capacity, a larger number (N) of slow sources (compared to the number of sources with $T_c = 1$) can be supported, provided that N remains below the buffer capacity.

Notice that for the results presented thus far, it is assumed that the controlled sources are synchronized ($c^1 = \cdots = c^N$) i.e: arrivals from the aggregate process occur in Binomially distributed batches with time constant equal to that of the individual sources. This may represent a worst case scenario in terms of queue performance. The impact of the synchronization of the different sources on the induced cell loss probabilities for different values of the buffer capacity (Q) is illustrated in Fig. 5. $N = 60$ sources are adaptively controlled; each of the individual sources has a time constant $T_c^j = 30$, $1 \leq j \leq 60$. The remaining parameters are set to $\lambda_1 = 0.94$, $\lambda_0 = 0.9$, $q_{th} = 30$ and $T_d = 30$. Several scenarios for the distribution of the initialization time of the individual sources are considered as follows:

- All sources are assumed to be synchronized, thus leading to an aggregate arrival process with $T_c = 30$ and $N = 60$.
- Initialization times of the sources are assumed to be $c^j = 1$, $1 \leq j \leq 30$ and $c^j = 15$, $31 \leq j \leq 60$, thus leading to an aggregate arrival process with $T_c = 15$ and $N = 30$.
- Initialization times of the sources are assumed to be $c^j = 1$, $1 \leq j \leq 20$, $c^j = 11$, $21 \leq j \leq 40$ and $c^j = 41$, $1 \leq j \leq 60$, thus leading to an aggregate arrival process with $T_c = 10$ and $N = 20$.
- Initialization times of the sources are assumed to be $c^j = j, 1 \leq j \leq 30$ and $c^j = j - 30, 31 \leq j \leq 60$ thus leading to an aggregate arrival process with $T_c = 1$ and $N = 2$.

Notice that the last case ($T_c = 1$ and $N = 2$) should not be confused with the classical assumption of unity time constant ($T_c = 1$ and $N = 60$) shown in Fig. 6. The overlap in effectiveness of the rate control for $T_c = 30$ is as explained before. As expected spreading the initialization times of the different sources leads to lower loss probabilities and consequently increased applicability of the adaptive rate control.

3 Adaptive Rate Control in the Presence of Diversified Propagation Delays: Fairness issues

In this section, the impact of the difference of propagation delays on the relative performance of individually controlled connections is considered. In order to facilitate the presentation, all controlled sources will be assumed to have a unity time constant ($T_c = 1$). As indicated in the introduction, the objective of this study is to quantify the impact of diversified propagation delays on the effectiveness of the most commonly proposed adaptive rate control scheme (source time constant equal to one), which is also expected to emphasize the most the unfairness issues based on the study in the previous section.

The model considered in this section, is shown in Fig. 7 where a number of sources share a common network access node. The access node is modeled by a finite buffer receiving deterministic service. Sources are divided into two groups: a group of N^l local sources which has a round-trip propagation delay of T_d^l and a group of N^r remote sources which has a round-trip propagation delay of T_d^r. The length of the update interval of the local (remote) sources T_u^l (T_u^r) is taken to be equal to the round-trip propagation delay of the local (remote) sources T_d^l (T_d^r). With minor changes, the presented analysis can be used when both the local and remote sources are updated at the same update interval ($T_u = T_d^r$). Numerical results will be derived for both cases in section 3.5.

It is further assumed that the adaptive rate control mechanism operates synchronously, that is sources within the same group switch to the low or high rate at the same instant. Therefore all sources within the same group are in the same state and thus the arrival process from the local (remote) sources can be represented by a two state process r^l (r^r), $r^l(r^r) \in \{0, 1\}$;

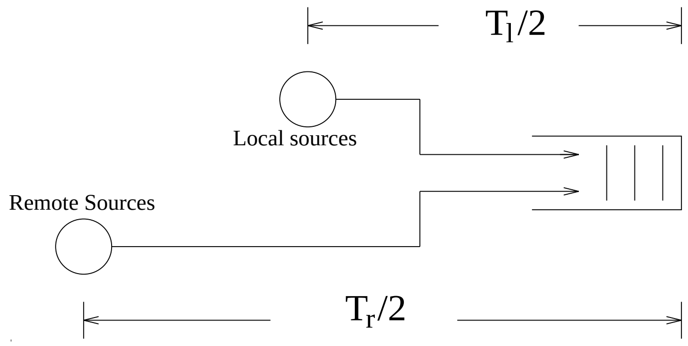

Figure 7: Queuing model for the study of the impact of the diversified propagation delays on the effectiveness of the adaptive rate control.

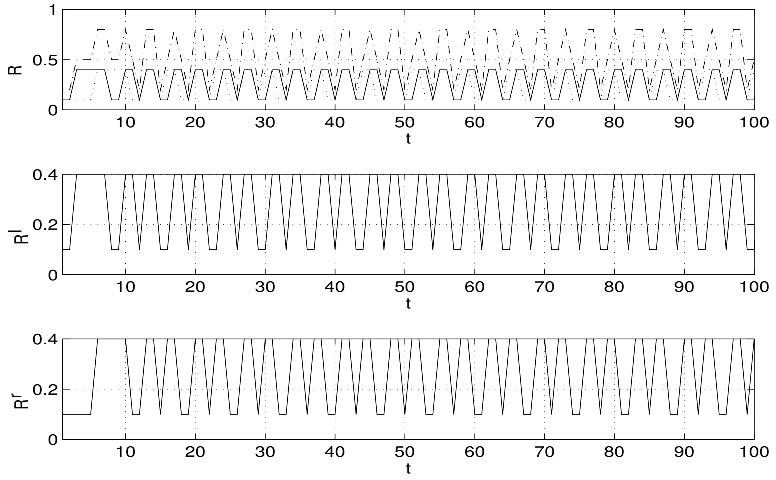

Figure 8: Simulation trace of the individual throughputs

sources transmit at a rate λ_0 (λ_1) when in state 0 (1). Transitions between the two states are controlled by the network state information. The aggregate traffic (arrival process) delivered to the network may be described by a two-dimensional process (r^l, r^r), the state space of which is $S_g = \{(0,0), (0,1), (1,0), (1,1)\}$.

If both the local and remote sources have the same propagation delays ($T_d^l = T_d^r$) and are updated with the same update interval, then due to the synchronous behavior of the considered adaptive rate control, the state space of the aggregate arrival process will be limited to $S_e = \{(0,0), (1,1)\}$. Consequently, the average arrivals from both sources should be equal at any time instant and hence the throughputs should be equal. However, due to the adaptive rate control, the total arrival process will oscillate between the two states $(0,0)$ and $(1,1)$. These oscillations has been shown to be a characteristic of any adaptive rate control with a non-increasing monotone control function of the network-state descriptor in [25] and that the system is stable in the sense that the arrival processes and the state of network-state descriptors will be confined to a small neighborhood of some operating point.

In the presence of unequal propagation delays, the state space of the aggregate arrival process is S_g. The throughput of the local (R^l) and remote processes (R^r) will depend on the time spent in the states $(0,1), (1,0)$. Again due to the synchronous and distributed nature of the considered algorithm when all sources are updated with the same update interval, it can be seen that whenever the local sources switch to some state i, the remote sources will switch to that same state i, $T_d^r - T_d^l$ time slots later. As a result, local and remote sources will achieve identical throughput, after some transient time period. This can be observed in the simulation trace in Fig. 8, where the network load is used as the network-state descriptor, infinite buffers are employed, $T_d^l = 2$, $T_d^r = 5$, $\lambda_1 = 0.4$ and $\lambda_0 = 0.1$. The arrival process of the remote sources lags that of the local sources by the difference in propagation delays (as can be seen from the lower two graphs in Fig. 8). However, the average throughputs are the same and the rate control scheme is fair in that sense. Connections considered in this work are assumed to have comparable life time durations and therefore transient effects due to the establishment and disconnection of new connections are not considered.

The presence of infinite capacity buffering guarantees that the above mentioned "lags" in the throughput will be "absorbed" and the resulting throughput will be equal to the arrival rate. This is not the case when finite buffers are employed. As a result, cell losses occur leading possibly to unequal throughputs and the issue of unfairness emerges.

Consider, for example, the realization of the buffer occupancy process under the adaptive rate control scheme in Fig. 9. The network buffer occupancy is taken to be the network's traffic descriptor and $\lambda_0 = 0$, that is, sources switch off to relieve the network congested state. At time instant t_1, the network-state indicator (buffer occupancy) is below the threshold (q_{th}), and a rate modulation cell is sent to the sources indicating that the network node is underloaded. Sources receive this cell after their respective propagation delay and respond by increasing their arrival rate. At time $t_2 = t_1 + T_d^l$, the higher local arrival rates reach the network node, and at $t_3 = t_1 + T_d^r$ the higher remote arrival rates reach the network node; the buffer occupancy maybe increasing. At time instant t_4, the buffer threshold is exceeded and a rate modulation signal is sent to the sources indicating that the network is overloaded. During the interval (I), the buffer capacity may be exceeded and losses may occur. Notice that losses may occur during that interval (I) from either of the two source groups since they are both active. After time instant $t_5 = t_4 + T_d^l$, arrivals occur only from the remote sources ($\lambda_0 = 0$) and therefore any cell losses that occur during the time interval (II), till remote sources cease to transmit, will be losses associated with the remote sources only. Thus, remote sources may suffer higher losses.

The potential for unfairness, due to distance, emphasizes the importance of the performance evaluation of adaptive rate control schemes. Since cell losses are also affected by the buffer management policy, the performance of the adaptive rate control schemes will be considered under several buffer management policies described in subsection 3.3. Note that in general, when two arrival streams have different arrival rates in any time interval (slot) and the buffer management policy treats all cells in the same manner, the number of cells lost is expected to be higher for the stream with the higher rate. When the propagation delays are equal, losses

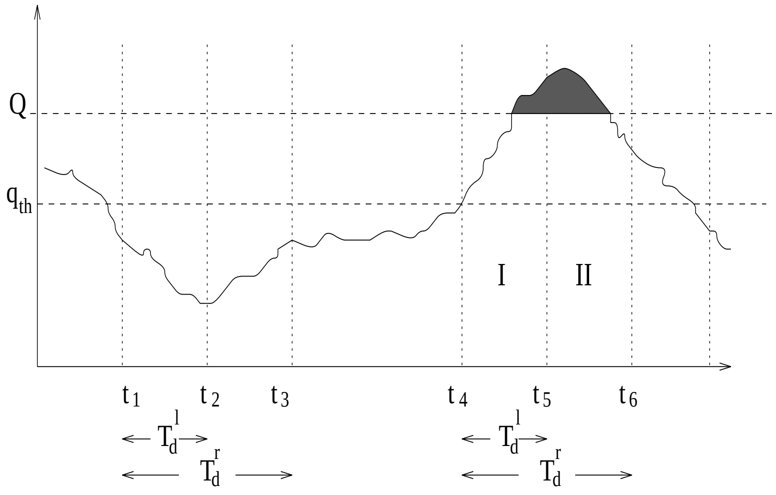

Figure 9: A realization of the network buffer

are expected to be equal since the arrival rates are equal at any time instant. This will be also shown later in section 3.5.

In the next subsections a queuing analysis is presented for the above system and the individual cell loss probabilities are derived.

3.1 Queuing Analysis

In this section, the queuing analysis is carried out in discrete-time. Time is slotted and a slot duration is equal to the transmission time of one cell. The propagation delay of the remote sources T_d^r is considered to be an integer multiple of that of the local sources, that is, $T_d^r = M \times T_d^l$, $M \in Z^+$, where Z^+ is the set of positive integers. Time is divided into frames each of length T_d^r slots; each frame is divided into M subframes, each of length T_d^l slots. Cell arrivals from both source groups arrive at a finite size network buffer of capacity Q and are served according to the FIFO service policy. If the number of cell arrivals over a slot exceeds the available buffer space, the buffer management policy determines which cells to be admitted to the queue. Several buffer management policies are considered in section 3.3.

Arrivals from the local (remote) sources are represented by a two state aggregate process $\{r^l\}, r^l \in \{0,1\}$ ($\{r^r\}, r^r \in \{0,1\}$), that will be referred to as the local (remote) arrival process. Let $F_i^l(k)$ ($F_i^r(k)$) denote the probability mass function (PMF) for the number of cells generated in each slot when the local (remote) process is in state $i, i \in \{0,1\}$. N_i^l (N_i^r) will denote the maximum number of local (remote) cell arrivals per slot from state i. State transitions for the local and remote arrival processes are governed by the two-level adaptive rate control mechanism as determined by the state of the network-state descriptor.

Let $\{q_k\}_{k\geq 0}$ be the buffer occupancy process embedded at subframe boundaries with state space $S^Q = \{0, 1, \cdots, Q\}$. Let q_{th} be the buffer threshold value indicating the network state as overloaded ($q \geq q_{th}$) or underloaded ($q < q_{th}$). Let $\{r^l_k\}_{k\geq 0}$ ($\{r^r_k\}_{k\geq 0}$) be the local (remote) arrival process embedded at the subframe boundaries with state space $S = \{0, 1\}$. Note that since the duration of the subframe is equal to the duration of the update interval of the local sources (T^l_d slots), state transitions of the process $\{r^l\}_{k\geq 0}$ occur only at *subframe* boundaries. Similarly, since the duration of the frame (M subframes) is equal to the update interval of the remote sources (T^r_d slots), state transitions of the process $\{r^r_k\}_{k\geq 0}$ occur only at *frame* boundaries. Notice also that due to the difference in propagation delays the state of process $\{r^l_k\}_{k\geq 0}$ at the beginning of subframe k is determined by the state of the buffer process at the beginning of subframe $k-1$, while the state of process $\{r^r\}_{k\geq 0}$ at the beginning of the same subframe is determined by the state of the buffer process at the beginning of subframe $(k - M)$. In order to obtain a system state description that evolves according to a Markov process embedded at subframe boundaries, the following two indicator processes are introduced to keep track of the state of the remote process at subframe boundaries:

- $\{I_k\}_{k\geq 0}$: it is an indicator process describing the index of subframe k, that is, its position within the current frame; its state space is $S^I = \{0, 1, \cdots, M-1\}$.
- $\{C_k\}_{k\geq 0}$: it is an indicator process— defined precisely below— embedded at subframe boundaries, which carries the state of the remote process at the first subframe (subframe 0) to the current subframe. It may change at subframe 0 and remains unchanged for the following $M - 1$ subframes; its state space is $S = \{0, 1\}$.

Thus the key processes evolve as follows:

$$I_{k+1} = (I_k + 1) \bmod M$$

$$r^l_{k+1} = \begin{cases} 1 & \text{if} \quad q_k < q_{th} \\ 0 & \text{if} \quad q_k \geq q_{th} \end{cases}$$

$$C_{k+1} = \begin{cases} 1 & \text{if} \quad q_k < q_{th} \ \text{ and } \ I_k = 0 \\ 0 & \text{if} \quad q_k \geq q_{th} \ \text{ and } \ I_k = 0 \\ C_k & \text{if} \quad I_k \neq 0 \end{cases}$$

$$r^r_{k+1} = \begin{cases} r^r_k & \text{if} \quad I_k \neq M-1 \\ C_k & \text{if} \quad I_k = M-1 \end{cases}$$

Given that $r^l_k = i$ and $r^r_k = j$ at the beginning of subframe k, the finite queue will evolve over subframe k under the i.i.d. batch arrival process with PMF obtained through the convolution of the PMFs F^l_i and F^r_j $(F(i,j,\cdot))$. It is easy to establish that the stochastic process $\{I_k, r^r_k, C_k, r^l_k, q_k\}_{k\geq 0}$, embedded at subframe boundaries, is a finite state Markov chain. Its state space is given by $S_p = S_0 \cup S_1 \cup S_2 \cup .... \cup S_{M-1}$, where

$$
\begin{aligned}
S_0 &= \{(I_1, r^r_1, C_1, r^l_1, q_1) : I_1 = 0, (r^r_1, C_1) \in S^j, r^l_1 \in S, q_1 \in S^Q\} \\
S_1 &= \{(I_1, r^r_1, C_1, r^l_1, q_1) : I_1 = 1, r^r_1 \in S, (C_1, r^l_1) \in S^j, q_1 \in S^Q\} \\
S_n &= \{(I_1, r^r_1, C_1, r^l_1, q_1) : I_1 = n, r^r_1 \in S, C_1 \in S, r^l_1 \in S, q_1 \in S^Q\}, \;\; 2 \leq n \leq M-1
\end{aligned}
$$

and $(I_1, r^r_1, C_1, r^l_1, q_1)$ denotes the current state of $(I_k, r^r_k, C_k, r^l_k, q_k)$. Note that S^p does not contain impossible states contained in the product space of the processes $\{I_k, C_k, r^r_k, r^l_k, q_k\}_{k\geq 0}$ and thus has reduced cardinality (memory requirements).

The transition probabilities of the above Markov chain can be expressed recursively as follows:

$$
p(I_1, r^r_1, C_1, r^l_1, q_1, I_2, C_2, r^r_2, r^l_2, q_2) = \begin{cases} 0 & \text{if } I_2 \neq (I_1 + 1) \bmod M \\ p_{I_1}(r^r_1, C_1, r^l_1, q_1, C_2, r^r_2, r^l_2, q_2) & \text{otherwise} \end{cases}
$$

$$
p_{I_1}(r^r_1, C_1, r^l_1, q_1, C_2, r^r_2, r^l_2, q_2) = \begin{cases} 0 & \text{if } (0 \leq I_1 \leq M-2), \\ & \quad (r^r_1 \neq r^r_2) \\ p_{I_1, r^r_1}(C_1, r^l_1, q_1, C_2, r^l_2, q_2) & \text{otherwise} \end{cases}
$$

$$
p_{I_1, r^r_1}(C_1, r^l_1, q_1, C_2, r^l_2, q_2) = \begin{cases} 0 & \text{if } (1 \leq I_1 \leq (M-2)), (C_1 \neq C_2) \\ p_{r^r_1}(r^l_1, q_1, r^l_2, q_2) & \text{otherwise} \end{cases}
$$

$$
p_{r^r_1}(r^l_1, q_1, r^l_2, q_2) = \begin{cases} 0 & \text{if } (q_1 < q_{th}), (r^l_2 = 0) \\ 0 & \text{if } (q_1 \geq q_{th}), (r^l_2 = 1) \\ p_{r^r_1, r^l_1}(q_1, q_2) & \text{otherwise} \end{cases}
$$

where $p_{r^r_1, r^l_1}(q_1, q_2)$ are the T^l_d-step transition probabilities from state q_1 to state q_2 for the finite queue, under the i.i.d batch arrival process specified by $F(r^l_1, r^r_1, \cdot)$. The one-step transition probabilities $\tilde{p}_{r^r_1, r^l_1}(q_1, q_2)$, $0 \leq q_1, q_2 \leq Q$, are given by:
For $0 \leq q_1 \leq Q$ and $max(0, q_1 - 1) \leq q_2 \leq Q - 1$,

$$
\tilde{p}_{r^r_1, r^l_1}(q_1, q_2) = F(r^l_1, r^r_1, q_2 - q_1 + 1) + F(r^l_1, r^r_1, 0) \cdot \mathbf{1}_{\{q_1 + q_2 = 0\}} \quad ,
$$

where $\mathbf{1}_{\{(q_1+q_2=0\}}$ is an indicator function that takes the value 1 if $q_1 + q_2 = 0$ and takes the value 0 otherwise.

For $0 \leq q_1 \leq Q$,

$$\tilde{p}_{r_1^r, r_1^l}(q_1, Q) = \sum_{l=Q-q_1+1}^{N} F(r_1^l, r_1^r, l) \quad ,$$

where $N = N^l_{r_1^l} + N^r_{r_1^r}$ denotes the maximum number of arrivals, as determined by the aggregate cell arrival process, when the local and remote arrival processes are in states r_1^l and r_1^r, respectively.

The multi-dimensional state-space of the process $(I_k, r_k^r, C_k, r_k^l, q_k)$ can be mapped lexicographically into a one dimensional space l_k. Due to the periodic evolution of I_k, the transition matrix of the one dimensional process l_k, $\mathbf{P}$, takes the canonical form of a periodic Markov chain of period M given by:

$$\mathbf{P} = \begin{bmatrix} 0 & \mathbf{P}_0 & 0 & \cdots & 0 \\ 0 & 0 & \mathbf{P}_1 & \cdots & 0 \\ \vdots & \vdots & \vdots & \ddots & \vdots \\ 0 & 0 & 0 & \cdots & \mathbf{P}_{M-2} \\ \mathbf{P}_{M-1} & 0 & 0 & \cdots & 0 \end{bmatrix} \tag{4}$$

where the matrices $\mathbf{P_i}, \mathbf{i} \in \{\mathbf{0}, \cdots, \mathbf{M-1}\}$ are those corresponding to state transitions from states $(i, \cdot, \cdot, \cdot, \cdot)$ to states $(j, \cdot, \cdot, \cdot, \cdot)$, where $j = (i+1) \bmod M$. Each $\mathbf{P_i}$ is of order $m_i \times m_{i+1}$ with $m_0 = 4(Q+1), m_1 = 4(Q+1), m_n = 8(Q+1), 2 \leq n \leq M-1$.

The stationary probabilities of the process l_k, or equivalently $\pi(I, r^r, C, r^l, i)$ can be obtained by utilizing theorem 7.1.6 in [26]. According to this theorem, any finite irreducible periodic Markov chain, with transition matrix such as in (4), has a unique stationary probability vector, $\mathbf{\Pi} = (\Pi_0 \cdots \Pi_{M-1})'$, given by:

$$\mathbf{\Pi} = \frac{1}{M} \left[\ \mathbf{\Pi}_0' \ \mathbf{\Pi}_1' \cdots \cdots \mathbf{\Pi}_{M-1}' \ \right]'.$$

where $\mathbf{\Pi}_i$ is the unique stationary probability vector obtained by solving $\mathbf{A}_i \mathbf{\Pi}_i = \mathbf{\Pi}_i$, with the normalizing condition $\mathbf{\Pi}_i' \mathbf{e} = 1$, where: $\mathbf{A}_i = \mathbf{P}_i \cdots \mathbf{P}_{M-1} \cdot \mathbf{P}_0 \cdots \mathbf{P}_{i-1}$ $(i = 1, \cdots, M-1)$, $\mathbf{A}_0 = \mathbf{P}_0 \cdots \mathbf{P}_{M-1}$ and $\mathbf{e}$ is a unity vector. Notice that each $\mathbf{A}_i$ is square and of order m_i. Thus, the stationary probability vector of the transition matrix $\mathbf{P}$ in (4), is obtained by solving M systems of m_i linear equations each, $0 \leq i \leq M-1$, the largest of which is composed of $8(Q+1)$ equations. This is instead of solving the larger system of order $|S| = 8(M-1)(Q-1)$. This effectively eliminates the dependence of the computational storage complexity on the ratio of the propagation delays $M = T_d^r/T_d^l$. Notice that since the Markov process is embedded at the subframe boundaries, the complexity is independent of T_d^l. Thus it is possible to solve for systems with both large local and remote propagation delays.

3.2 Per-session Cell Loss Probability

In this section, the cell loss probability of an arbitrary cell from the local arrival process is derived. The cell loss probability for the remote arrival process and the overall cell loss probability can be derived in a similar fashion.

In the following, let r^l, r^r be states of the local and remote arrival processes at the beginning of the current subframe, respectively. Let i be the buffer state at the beginning of the k^{th} slot in the subframe. Let $w_l(r^l, r^r, i, k), 1 \leq k \leq T_d^l$ be a random variable describing the number of local cells lost over the period starting from the beginning of the k^{th} slot till the end of the current subframe (over a period of $T_d^l - k$ slots). Clearly, $w_l(r^l, r^r, i, 1)$ describes the number of losses over the period of the subframe. It can be easily shown that the loss probability of the local sources (L_l) can be derived in terms of the expected value of $w_l(.,.,.,.)$, $\overline{w_l}(.,.,.,.)$, as follows:

$$L_l = \frac{\sum_{(n,r^r,C,r^l,i)\in S_p} \pi(n, r^r, C, r^l, i)\overline{w_l}(r^r, r^l, i, 1)}{\sum_{(n,r^r,C,r^l,i)\in S_p} \pi(n, r^r, C, r^l, i)\lambda_{r^l} T_d^l}$$

Let w_1 be a random variable describing the number of local cells lost during the k^{th} slot. The random variables $w_l(r^l, r^r, i, k)$ and their expected values can be derived recursively by noting that the number of cells lost starting from the k^{th} slot in the current subframe till the end of the subframe is equal to the number of cells lost over the k^{th} slot plus the number of cells lost from the beginning of the $(k+1)^{st}$ slot till the end of the subframe, as follows:

For $i \in \{0, \cdots, Q\}$, $1 \leq k \leq T_d^l - 1$:

$$w_l(r^l, r^r, i, k) = \begin{cases} 0 + w_l(r^l, r^r, j, k+1) & \text{if } i \xrightarrow{1} j, \;\; j \neq Q \\ m + w_l(r^l, r^r, Q, k+1) & \text{if } w_1 = m, \;\; 0 \leq m \leq N_{r^l}^l \end{cases}$$

$$w_l(r^l, r^r, i, T_d^l) = \begin{cases} m & \text{if } w_1 = m, \;\; 0 \leq m \leq N_{r^l}^l \\ 0 & \text{otherwise} \end{cases}$$

Let $p_l(m, i, r^l, r^r)$ denote the probability that $w_1 = m$, the buffer occupancy is i and the arrival processes are in states r^l, r^r, respectively. The probabilities $p_l(m, i, r^l, r^r)$, needed for the evaluation of $\overline{w}(.,.,.,.)$, depend on the buffer management policy and will be derived in the next subsection.

3.3 Buffer management Policies

The buffer management policy determines the number of cells from each of the local and the remote arrival processes which are discarded over any slot. It is therefore necessary to consider the impact of the buffer management policy on the per-session performance in conjunction with the rate control scheme.

Let i denote the buffer state at the beginning of the current time slot. It is assumed that the cell receiving service during that time slot leaves the queue immediately at the beginning of the slot and thus the remaining buffer capacity that can be allocated to arriving cells during the current time slot is $Q - i + 1$. Let k_l and k_r be the number of local and remote cells arrived during the current time slot, respectively. The local process cell discarding probabilities $p_l(m, i, r^l, r^r)$, introduced in subsection (3.2), can be evaluated as:

$$p_l(m, i, r^l, r^r) = \sum_{k_l=0}^{N^l_{r^l}} \sum_{k_r=0}^{N^r_{r^r}} p_l[(m, i, r^l, r^r)|(k_l, k_r)] F^l_{r^l}(k_l) F^r_{r^r}(k_r)$$

where the conditional probabilities $p_l[(m, i, r^l, r^r)|(k_l, k_r)]$ are determined by the adopted buffer management policy. A number of policies are considered in the following subsections.

3.3.1 Equal Remaining Capacity (ERC) Policy

According to this buffer management policy, the remaining number of available buffer positions at any time slot is split equally between the two arrival processes, or equivalently the buffer management policy assigns every other position to one of the two contending processes. If some of the buffer positions allocated to one of the two processes are not used, they may be utilized by the other arrival process. If the number of remaining buffer positions is an odd integer, then the remaining buffer positions can not be split equally between the two arrival processes. The remaining buffer position in this case may be randomly assigned to any of the two processes or may always be assigned to the same process; the former case is considered here. Consider the following quantities which are used in the derivation of cell losses:

$$\begin{array}{ll} s = (Q-i+1)/2 & \text{if } (Q-i+1)/2 \in Z^+ \\ s_u = \lceil (Q-i+1)/2 \rceil & \text{if } (Q-i+1)/2 \notin Z^+ \\ s_w = \lfloor (Q-i+1)/2 \rfloor & \text{if } (Q-i+1)/2 \notin Z^+ \end{array}$$

The number of cells lost from the local arrival process (l_l) can be determined by:
For $k_l \in \{0, \cdots, N^l_{r^l}\}, k_r \in \{0, \cdots, N^r_{r^r}\}, i \in \{0, \cdots, Q\}$:

For $(Q-i+1)/2 \notin Z^+$:

$$l_l = \begin{cases} \lceil k_l - s_w - [s_u - k_r]^+ \rceil^+ & \text{with probability } 0.5 \\ \lceil k_l - s_u - [s_w - k_r]^+ \rceil^+ & \text{with probability } 0.5 \end{cases}$$

For $(Q-i+1)/2 \in Z^+$:

$$l_l = \lceil k_l - s - [s - k_r]^+ \rceil^+$$

The computation of the probabilities $p_l[(m,i,r^l,r^r)|(k_l,k_r)]$ follows easily. The number of cells lost from the remote sources l_r and the probabilities $p_r[(m,i,r^l,r^r)|(k_l,k_r)]$ can be found similarly.

3.3.2 Random Allocation (RA) Policy

According to the random allocation policy, two bounds on the number of local (remote) cells that may be lost during the current time slot are defined: an upper bound m_u and a lower bound m_w. The number of local (remote) cells lost m^l (m^r) is uniformly distributed between the two bounds. Since the number of local cells lost can not exceed either of the number of local cells arrived during the slot or the total number of cells lost, then the upper bound on local cells lost m_u^l is $\min\{k_l, k_l + k_r - (Q-i+1)\}$. The lower bound m_w^l is $\max\{0, k_l - (Q-i+1)\}$, where $k_l - (Q-i+1)$ is the total number of cells lost, $k_l + k_r - (Q-i+1)$, minus the maximum number of cells that can be lost from the remote sources (k_r). Thus:

$$p_l[(m,i,r^l,r^r)|(k_l,k_r)] = \begin{cases} \frac{1}{m_u^l - m_w^l + 1} & \text{if } k_l + k_r \geq (Q-i+1+m),\ \ m_w^l \leq m \leq m_u^l \\ 0 & \text{otherwise} \end{cases}$$

and $p_r[(m,i,r^l,r^r)|(k_l,k_r)]$ can be found similarly.

3.3.3 Fixed Distribution policy (FD) Policy

This policy favors certain loss patterns over others. As with the random policy, an upper bound m_u and a lower bound m_w are identified. However, instead of the uniform distribution of losses between the two bounds in the random policy, a specific distribution $g(m), m_w \leq m \leq m_u$ is identified and cell losses are distributed accordingly. Thus:

$$p_l[(m,i,r^l,r^r)|(k_l,k_r)] = \begin{cases} g(m) & \text{if } k_l + k_r \geq (Q-i+1+m),\ \ m_w^l \leq m \leq m_u^l \\ 0 & \text{otherwise} \end{cases}$$

$p_r[(m,i,r^l,r^r)|(k_l,k_r)]$ can be found similarly. $g(m)$ may be chosen to minimize the difference between losses for the remote and local processes. A simple $g(m)$ is considered in this work, where losses are split equally, if possible, whenever they occur. The policy considered distributes the cell losses equally between the two processes. Assuming that a total of $l' = k_l + k_r - (Q - i + 1)$ cells will be lost in the current slot, the policy operates as follows: For $l'/2 \in Z^+$:

$$l_l = \min\{\max(l'/2, m_w), m_u\}$$

For $l'/2 \notin Z^+$:

$$l_l = \begin{cases} \min[\max(\lceil l'/2 \rceil, m_w), m_u] & \text{with probability } 0.5 \\ \min[\max(\lfloor l'/2 \rfloor, m_w), m_u] & \text{with probability } 0.5 \end{cases}$$

The computation of the probabilities $p_l[(m, i, r^l, r^r)|(k_l, k_r)]$ follows easily. The number of cells lost from the remote sources l_r and the probabilities $p_r[(m, i, r^l, r^r)|(k_l, k_r)]$ can be found similarly.

3.4 Equal Update Intervals

The analysis developed earlier can be simply used when both the local and remote sources are updated at the same update interval $T_u = T_d^r$. In this case, both the local and remote process transitions occur at frame boundaries. The evolution of the local arrival process is as shown below while all other processes evolve as before.

$$r_{k+1}^l = \begin{cases} 1 & \text{if } q_k < q_{th} \quad \text{and} \quad I_k = 0 \\ 0 & \text{if } q_k \geq q_{th} \quad \text{and} \quad I_k = 0 \\ r_k^l & \text{otherwise} \end{cases} \tag{5}$$

The system's steady state probabilities and consequently the cell loss probabilities are derived as above.

3.5 Numerical Results and Discussion

For the results derived in this section, both the local and remote arrival processes are assumed to follow a binomial distribution with parameters $N_0, \lambda_0/N_0$ when in state 0 and with parameters $N_1, \lambda_1/N_1$ when in state 1.

The effect of the ratio of the propagation delays M on the cell loss probability is shown in Fig. 10 under the ERC policy where different update intervals are used, $\lambda_h = 0.8$, $\lambda_l = 0.10$, $N_0 = 1$, $N_1 = 20$, $Q = 60$, $q_{th} = 50$ and $T_d^l = 2$. The unfairness is also clear from Fig. 11, where the ratio of the remote loss probabilities to the local loss probabilities increases as M increases. The effectiveness of the FD policy and the RA policy over the ERC policy in reducing the differences in cell loss probabilities becomes apparent as M increases.

The throughputs obtained by the FD policy is shown in Fig. 12. Note that as M increases, the ratio between the update intervals ($T_d^r/T_d^l = M$) increases and the unfairness as expressed by the differences in throughputs increase. The throughputs obtained by the RA and ERC policies are almost identical to that obtained by the FD policy and are not plotted. This is expected, since the buffer management policies primarily control the losses. For the above parameters, losses are in small orders of magnitude and the throughputs are mainly controlled by the time individual sources operate at the different access rates. This can be seen from Fig. 13, for equal update intervals, where the differences in throughputs are negligible and are mainly due to the losses.

Fig. 14 shows the loss probability for the ERC policy under equal update intervals ($T_u = T_d^r$) for the same parameters considered before. Although the ratio of remote to local cell losses tend to be smaller than when unequal update intervals is employed (Fig. 10), the overall losses tend to be higher due to the lax control over the local sources. (local sources are updated at longer intervals (T_d^r) than before (T_d^l)).

Fig. 15 shows that the unfairness increases as the difference between λ_h and λ_l increases. This can also be seen from Fig. 16 where the ratio of remote and local loss probabilities are shown. The dependence of the unfairness on the choice of the overall parameters in the system can be seen by contrasting Fig. 17 where $\lambda_h = 0.49$, $M = 4$, $N_0 = 10$, $N_1 = 10$, $Q = 40$, $q_{th} = 20$ and $T_d^l = 10$ with Fig. 15 where $\lambda_h = 0.8$, $M = 4$, $N_0 = 10$, $N_1 = 20$, $Q = 60$, $q_{th} = 50$ and $T_d^l = 2$. In the former figure (Fig. 17), the loss probabilities of the local and the remote processes are almost equal.

The above results show that it is necessary to carefully choose the update interval scheme (identical or non-identical) as well as the parameters of the rate control scheme; operating the system in a region of high losses under unequal update intervals increases the difference between the cell loss probabilities suffered by the local and remote sources. It is clearly seen that these differences decrease as the system is operated in a low loss region.

Finally, it should be noted that the results presented in this section are derived for sources with time constant equal to 1 ($T_c = 1$). Earlier results — presented in section 2.4 — indicated that an increased time constant induces lower cell loss probabilities (assuming $Q > N$). It is therefore expected that in this latter case the difference in cell loss probabilities due to diversified propagation delays will be rather insignificant, provided that the system operates in a low cell loss region.

4 Concluding Remarks

In this work, some of the performance issues related to a simple two-level (Binary) adaptive rate control scheme in a high-speed environment are considered. Appropriate queuing models are formulated and analyzed to investigate two key performance issues for adaptive rate control schemes.

First, the impact of the ratio between the network and source speeds on the effectiveness of the adaptive rate control is considered. Unlike previous studies, a queuing model for an adaptive rate control scheme incorporating slow arrival processes that deliver cells with a certain time constant is considered. An efficient technique is developed for the computation of the induced cell loss probabilities. Numerical results show that the performance of an adaptive feedback-based rate control scheme may be substantially underestimated if the time constant of a slow arrival process is assumed to be one ($T_c = 1$), as in previous studies. Numerical results also show that the effectiveness of the adaptive rate control scheme depends heavily on the relationship between the number of the controlled sources and the available buffer capacity. The results point to the existence of a *batch-absorption buffer capacity value* beyond which the effectiveness of the adaptive rate control will increase as the source time constant increases. Finally, a significant conclusion from the presented results is that for a fixed cell loss probability and (sufficiently large) fixed buffer capacity, a larger number (N) of slow sources (compared to the number of sources with $T_c = 1$) can be supported provided that N remains below the buffer capacity.

Second, the impact of the difference in propagation delays and update intervals on the performance seen by two groups of sources with vastly different propagation delays is considered. Although in the presence of infinite capacity buffers and equal update intervals, an adaptive rate control scheme leads to equal distribution of bandwidth between the competing connections— irrespective of their propagation delays— it is shown that it leads to unequal distribution of cell loss when finite capacity buffers are considered. An efficient technique is developed for the computation of the cell loss probabilities of the local and remote connections; the dimensionality of the formulated model is independent of the associated propagation delays. Numerical results show that when different update intervals are used, increased unfairness and significant differences in the relative performance may be seen by the different sources as the ratio between the propagation delays increases. It is further shown that the relative performance seen by the different groups largely depends on the choice of the update intervals (identical or un-identical), as well as the choice of the rate control parameters. In particular, it is shown that the difference in performance decreases (increases) if the rate control system is operated in a low (high) loss region.

References

[1] J. Bae and T. Suda. Survey of traffic control schemes and protocols in ATM networks. In *Proceedings of the IEEE*, pages 170–189, 1991.

[2] F. Bonomi and K. W. Fendick. The rate-based flow control framework for the available bit rate ATM service. *IEEE Network Magazine*, March 1995.

[3] G. Dobrowski. ATM forum specification update. In *53 Bytes: The ATM Forum Newsletter*, volume 3. The ATM Forum, Jan 1995.

[4] P. Skelly, G. Pacifici, and M. Schwartz. A cell and burst level control framework for integrated video and image traffic. In *Infocom'94*, pages 346–354, Toronto, Canada, 1994.

[5] A. Tanenbaum. *Computer Networks.* Prentice Hall, 1989.

[6] K. K. Ramakrishnan and R. Jain. A binary feed back scheme for congestion avoidance in computer networks. *ACM Transactions on Computer Systems*, pages 158–181, May 1990.

[7] V. Jacobson. Congestion avoidance and control. *ACM Computer Communication Review*, pages 314–329, Aug 1988.

[8] A. Atai and J. Hui. Rate-based feedback traffic controller for ATM networks. In *ICC'94*, pages 1605–1615, New Orleans, 1994.

[9] R.S. Pazhyannur and R. Agrawal. Analytical and numerical results for feedback based flow control of B-ISDN/ATM networks with signifcant propagation delays. In *Infocom'95*, pages 738–745, Boston, 1995.

[10] M. Murata N. Wakamiya, K. Baba and H. Miyahara. Performance analysis of traffic control methods in multimedia ATM lan. In *Infocom'95*, pages 1027–1036, Boston, 1995.

[11] D.D. Clark A. Charny and R. Jain. Congestion control with explicit rate indication. In *ICC'95*, pages 1954–1963, Seattle, WA, 1995.

[12] N. Giroux and D. Chiswell. ATM layer traffic management functions and procedures. In *Engineer Conference Notes, Networld+Interop'95*, Las Vegas, Nevada, Mar 1995.

[13] N. Yin and M. Hluchyi. On closed-loop rate control for ATM cell relay networks. In *Infocom'94*, pages 99–108, Toronto, Canada, 1994.

[14] M. Murata K. Kawahara, Y. Oie and H. Miyahara. Performance analysis of reactive congestion control for ATM networks. *IEEE Trans. Commun.*, pages 651–661, May 1995.

[15] A. Kolarov and G. Ramamurthy. Comparison of congestion control schemes for abr service in ATM local area networks. In *IEEE GLOBECOM'94*, pages 913–918, San Francisco, CA, 1994.

[16] L. G. Roberts. Can abr service replace vbr service in ATM networks. In *Engineer Conference Notes, Networld+Interop'95*, Las Vegas, Nevada, Mar 1995.

[17] N. Yin and M. Hluchyi. A dynamic rate control mechanism for source coded traffic in a fast packet network. *IEEE J. Select. Areas Commun., Vol. 9, No. 7*, pages 1003–1012, Sep 1991.

[18] H. Bradlow D. Hughes. Congestion control in ATM network. In *ITC 13 (Teletraffic and Datatraffic in a Period of Change)*, pages 835–840, Copenhagen, Denmark, Jun 1991.

[19] P. Newman. Backward explicit congestion notification for ATM local area networks. In *GLOBECOM'93*, pages 719–723, Switzerland, 1993.

[20] Y. T. Wang and B. Sengupta. Performance analysis of a feedback congestion control policy under non-negligible propagation delay. In *Sigcomm'91*, pages 149–157, Zurich, Switzerland, Sep 1991.

[21] D. Chiu and R. Jain. Analysis of the increase and decrease algorithms for congestion avoidance in computer networks. *Computer Networks and ISDN Systems*, pages 1–14, 1989.

[22] A. Mukherjee and J. C. Strikwerda. Analysis of dynamic congestion control protocols - a fokker-planck approximation. In *Sigcomm'91*, pages 159–169, Zurich, Switzerland, Sept 1991.

[23] I. Stavrakakis. Statistical multiplexing of correlated slow traffic sources. In *GLOBECOM'92*, Orlando, FL, 1992.

[24] R. Landry and I. Stavrakakis. Non-deterministic periodic packet streams and their impact on a finite-capacity multiplexer. In *Infocom'94*, Toronto, Canada, 1994.

[25] M. A. Rodrigues K. W. Fendick and A. Weiss. Analysis of a rate-based control strategy with delayed feedback. *Computer Communication Review*, pages 136–148, Oct 1992.

[26] J. Hunter. *Mathematical Techniques of Applied Probability, Discrete Time Models: Techniques and Applications*, volume II. Academic Press, 1983.

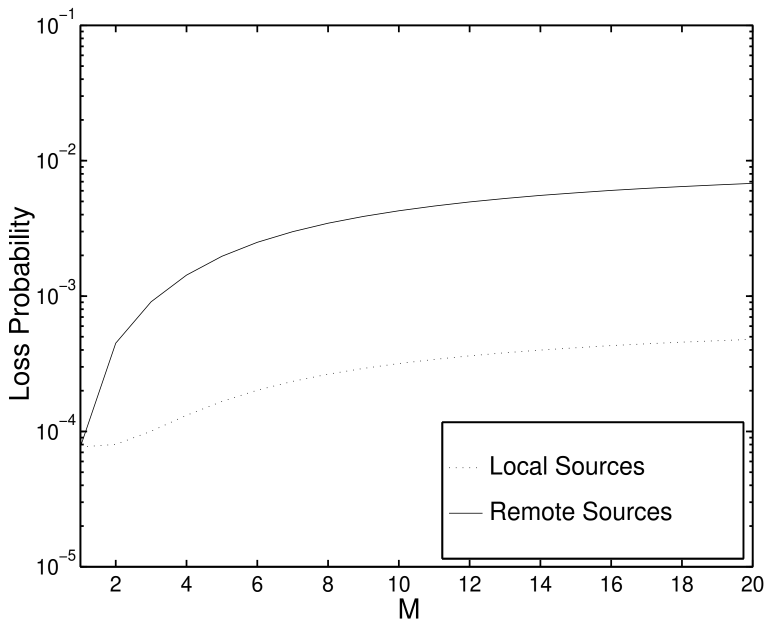

Figure 10: ERC Policy, unequal update intervals

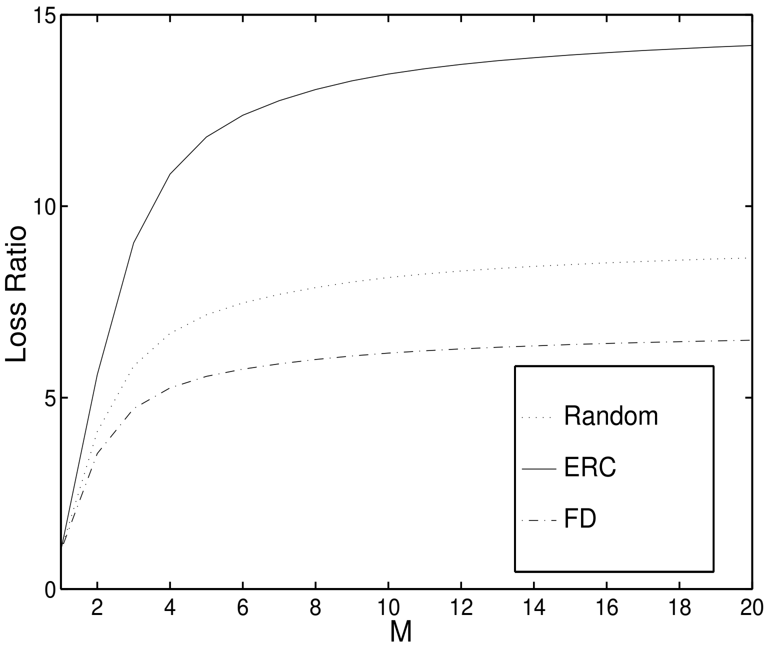

Figure 11: Ratio of remote cell losses to local cell losses

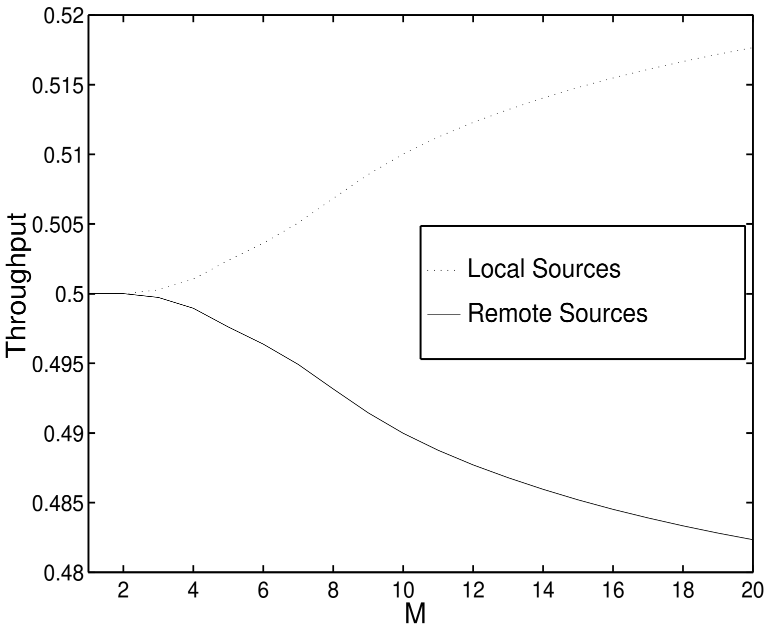

Figure 12: FD Policy, unequal update intervals

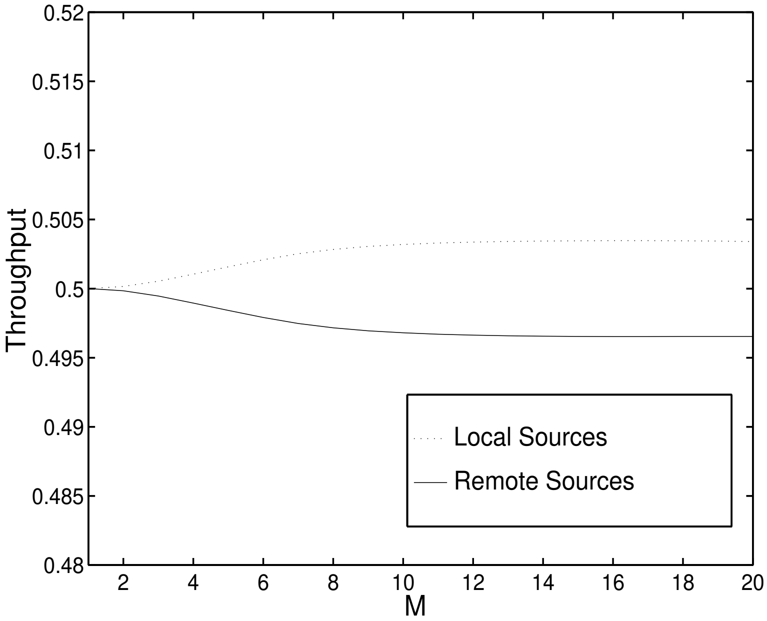

Figure 13: FD Policy, equal update intervals

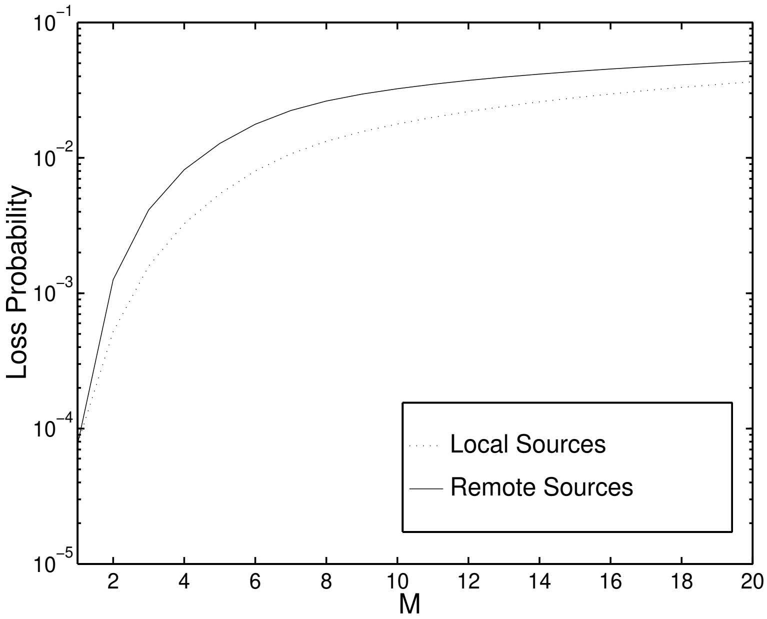

Figure 14: ERC Policy, equal update intervals

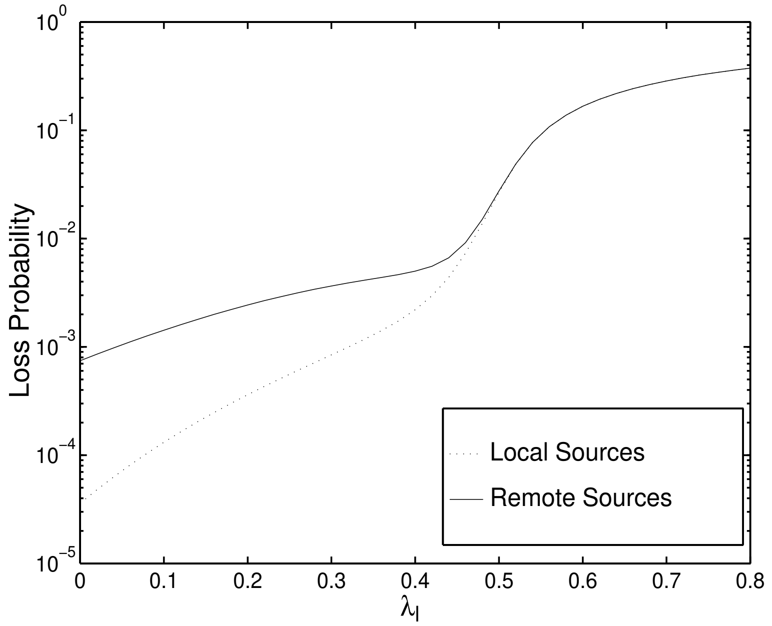

Figure 15: Effect of changing λ_l, unequal update intervals

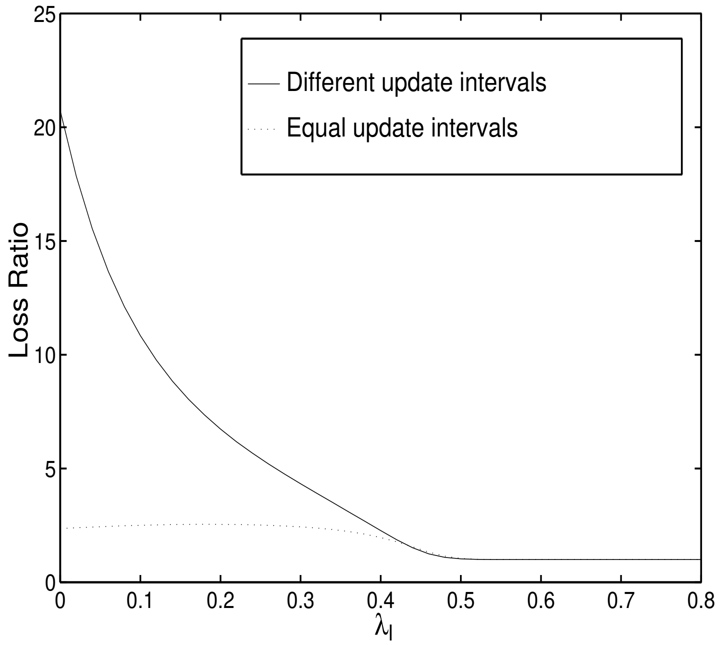

Figure 16: Ratio of remote to local cell losses (ERC policy)

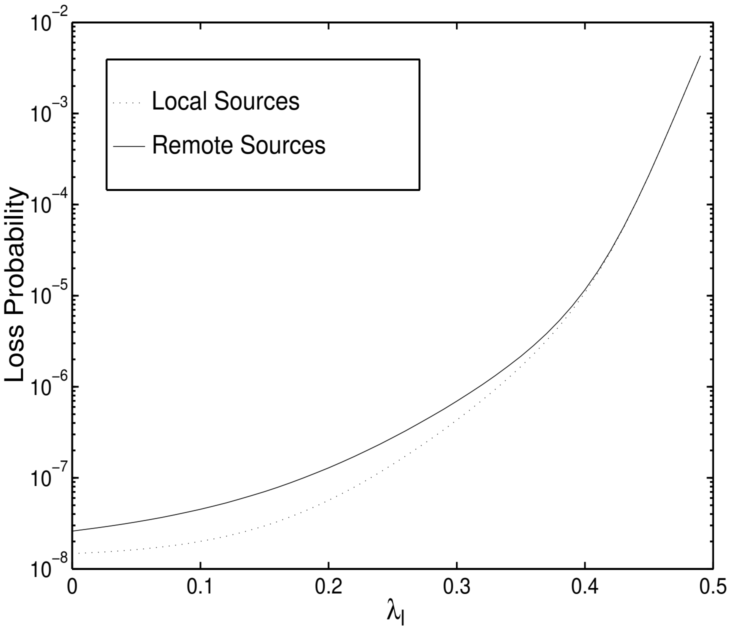

Figure 17: Effect of changing λ_l, unequal update intervals